Cooperatively surrounding control for multiple Euler–Lagrange systems subjected to uncertain dynamics and input constraints*

Liang-Ming Chen(陈亮名), Yue-Yong Lv(吕跃勇), Chuan-Jiang Li(李传江)†, and Guang-Fu Ma(马广富)

School of Astronautics, Harbin Institute of Technology, Harbin 150001, *China*

(Received 11 May 2016; revised manuscript received 27 June 2016; published online 25 October 2016)

In this paper, we investigate cooperatively surrounding control (CSC) of multi-agent systems modeled by Euler–Lagrange (EL) equations under a directed graph. With the consideration of the uncertain dynamics in an EL system, a backstepping CSC algorithm combined with neural-networks is proposed first such that the agents can move cooperatively to surround the stationary target. Then, a command filtered backstepping CSC algorithm is further proposed to deal with the constraints on control input and the absence of neighbors' velocity information. Numerical examples of eight satellites surrounding one space target illustrate the effectiveness of the theoretical results.

Keywords: surrounding control, Euler–Lagrange system, backstepping

PACS: 87.19.lr, 02.30.Yy, 45.80.+r **DOI:** 10.1088/1674-1056/25/12/128701

1. Introduction

Recently, the cooperative controls of multi-agent systems have drawn a large amount of attention in many fields, such as spacecraft formation flying,[1] coordination of wireless sensor network,[2] and synchronization of autonomous robots.[3] In particular, leaderless consensus,[4–7] leader-following tracking,[8–12] and distributed containment with multiple leaders[13–15] have received most attention in the field of cooperative control.

Unlike the distributed containment control problem where the cooperative containment control algorithm is designed for followers such that all the followers converge into the convex hull spanned by multiple leaders,[14] the cooperatively surrounding control (CSC) problem is considered as an inverse of the distributed containment control problem where the CSC algorithm is designed for agents such that all the agents move cooperatively to surround the target or multiple targets.[16] With this background, the CSC is quite suitable for many practical space applications such as orbital debris removal, on-orbit refueling, reconnaissance, and maintenance.[17,18] However, the relationship between the agents and the target in the CSC problem is usually non-cooperative because the target could not initiatively send any state information to the agents.[19] The non-cooperativeness poses challenges for the agents' controller design in the CSC problem. Therefore, it is of great significance to conduct further research in the CSC problem. However, there are few results about this issue to date. Under a decentralized estimation-and-control framework, in Ref. [20] the CSC problem for first-order integrator linear systems was studied on the assumption that the followers were placed within a circle and a leader can communicate with at least one follower initially. In Ref. [21] the CSC problem was studied for first-order integrator linear systems under an undirected graph, where a CSC law is designed for agents such that all agents could encircle the dynamic targets by calculating the average position of the targets. There are three limitations in Ref. [21]: (i) the number of targets must be the same as the number of the agents; (ii) the working modes between agents and targets are collaborative because the targets' velocity information is available to the agents, and each agent can always be connected to a target; (iii) all the agents finally form a formation of the same shape but larger than that of the targets. In Ref. [22] the results of Ref. [21] were extended to the second-order integrator linear system. Based on cyclic pursuit strategies, a special case of CSC problem was also studied in Refs. [23] and [24]. However, in the above Refs. [20]–[24] the practical constraints in systems were not considered, such as the uncertain dynamics and input saturation, the difficulty of real-time and bidirectional information interaction among agents, and the communication burden of relative velocity information.

Uncertain dynamics exists in many practical systems for the disturbance and the unmodeled dynamics.[25] By comparing known parameters and unknown parameters, the synchronization control of two different chaotic systems was investigated in Ref. [26]. To deal with uncertain dynamics in the system, the backstepping design method was used in Ref. [27] to realize the distributed tracking control of nonlinear stochastic multi-agent systems under a directed graph. In Ref. [28] a distributed consensus tracking control problem under an undirected graph was investigated, in which the function approx-

*Project supported by the National Basic Research Program of China (Grant No. 2012CB720000) and the National Natural Science Foundation of China (Grant Nos. 61304005 and 61403103).

†Corresponding author. E-mail: lichuan@hit.edu.cn

© 2016 Chinese Physical Society and IOP Publishing Ltd

imation using neural networks was employed to compensate for the unknown dynamics induced from controller design procedure. With the limitation to controllers and actuators, input constraints, such as magnitude, rate and bandwidth limitations, cannot be ignored in practice.[29,30] With the consideration of input saturation, the robust stabilization of state delayed discrete-time Takagi–Sugeno fuzzy system is studied in Ref. [31] by using the anti-windup fuzzy design method. In Ref. [32] the control of an unmanned air vehicle was studied, where a command filter was used to handle the intermediate state and the surface with magnitude, rate and bandwidth limitations. However, the reports in which the uncertain dynamics and input constraints are considered simultaneously in the CSC problem are few until now.

The objective of this paper is to study the CSC problem for a multi-agent system modeled by Euler–Lagrange (EL) equations under a directed graph. As many physical systems are inherently nonlinear in practice, it is significant to describe the model of agents by nonlinear equation. The EL system is a special case of the second-order nonlinear system which can be used to represent a large class of physical mechanical systems, such as underwater vehicles,[33] robotic manipulators,[34] and flying spacecrafts.[35] The relationship between target and agents is non-collaborative, in which the position of the stationary target is only available to a portion of agents. With the consideration of uncertain dynamics in the EL system, by incorporating neural-networks (NN) technique into backstepping control design framework, a backstepping CSC algorithm is first investigated such that all agents move cooperatively to surround the stationary target. Then, by decoupling the design of the controllers for the backstepping iterations and derivative output of the command filter, we further develop a command filtered backstepping CSC algorithm to cope with the constraints on control input and the absence of neighbors' velocity information. Numerical examples of eight satellites surrounding one space target illustrate the effectiveness of the obtained theoretical results.

To sum up, compared with those of other references studying the CSC problem, the main advantages of this paper are: i) the agents' dynamics used in this paper are for nonlinear EL systems; ii) the uncertain dynamics and input constraints in systems are considered; iii) the numbers of targets and surrounding formation are not constrained; iv) the communication topology between agents is a directed graph without using the relative velocity information.

2. Preliminary and problem statement

Some basic preliminaries about the EL systems, graph theory and problem statement will be introduced in this section.

2.1. EL dynamics

EL system is a special case of the second-order nonlinear system which can be used to represent a large class of physical mechanical systems. The dynamic equation of Euler–Lagrange system can be described as

$$M_i(q_i)\ddot{q}_i + C_i(q_i,\dot{q}_i)\dot{q}_i + g_i(q_i) = \tau_i + \omega_i, \tag{1}$$

where $q_i \in \mathbb{R}^p$ is the vector of generalized coordinates of the i-th agent, p is the degree of freedom in system, $M_i(q_i) \in \mathbb{R}^{p\times p}$ is the symmetric positive definite inertia matrix, $C_i(q_i,\dot{q}_i)\dot{q}_i \in \mathbb{R}^p$ is the Coriolis and centrifugal force, $g_i(q_i) \in \mathbb{R}^p$ is the vector of gravitational force, $\tau_i \in \mathbb{R}^p$ represents the control input, $\omega_i \in \mathbb{R}^p$ denotes the external disturbance. In this study, we assume that $M_i(q_i)$, $C_i(q_i,\dot{q}_i)$, and $g_i(q_i)$ have uncertain dynamics and are all unknown for the controller design. For most of the physical mechanical systems described by EL dynamics, the following properties[8] are satisfied and will be used for the controller design and the stability analysis.

Property 1 $\dot{M}_i(q_i) - 2C_i(q_i,\dot{q}_i)$ is skew symmetric, that is, for $\forall x_i \in \mathbb{R}^p$, $x_i^{\mathrm{T}}[\dot{M}_i(q_i) - 2C_i(q_i,\dot{q}_i)]x_i = 0$ is set up.

Property 2 Matrix $M_i(q_i)$ is bounded by $k_{\underline{m}} I_p \le M_i(q_i) \le k_{\bar{m}} I_p$ where $k_{\underline{m}}$ and $k_{\bar{m}}$ are the positive constants, and I_p denotes the $p \times p$ identity matrix.

The following assumption about the external disturbance ω_i is made for the convenience of controller design and stability analysis.

Assumption 1 The external disturbance ω_i is bounded by $\|\omega_i\| \le \omega_{Mi}$ where ω_{Mi} is a positive constant.

2.2. Graph theory

The directed graph $G = (V, \varepsilon, A)$ is used to describe the information interchange between the n agents. $V = \{v_1, \ldots, v_n\}$ represents the set of nodes. $\varepsilon \subseteq V \times V$ is a set of edges, in which $(v_i, v_j) \in \varepsilon$ represents that agent i can send information to agent j, but not *vice versa*. Here, node i is a neighbor of node j and the set of all neighbors of node i is denoted as N_i. $A = [a_{ij}] \in \mathbb{R}^{n\times n}$ is the weighted adjacency matrix of G, where $a_{ii} = 0$, $a_{ij} > 0$ if and only if $(v_j, v_i) \in \varepsilon$, and $a_{ij} = 0$ if $(v_j, v_i) \notin \varepsilon$. A directed path from node v_{i_1} to v_{i_k} is a sequence of ordered edges $v_{i_1}, \ldots, v_{i_k}$, which satisfy $(v_{i_s}, v_{i_{s+1}}) \in \varepsilon$. A directed graph is said to have a spanning tree if there exists at least one node having a directed path to all the other nodes. The Laplacian matrix of graph G is defined as $L = D - A$, where $D = \mathrm{diag}(d_1, \ldots, d_n)$ is a diagonal matrix and $d_i = \sum_{j=1}^{n} a_{ij}$.

2.3. Problem statement

With the consideration of a system composed of a static target (labeled as 0) and N agents (labeled as $M = \{1, \ldots, N\}$) with EL dynamics (1), the objective of this study is to design a CSC algorithm $\tau_i(q_i, \dot{q}_i, q_j, \dot{q}_j), j \in N_i$ for each agent $i (\forall i \in M)$

under a directed graph such that all agents can move collectively to encircle the target with desired formation configuration, which means $\lim_{t\to\infty}(q_i - q_0 - \delta_{i0}) = 0$, where δ_{i0} is the desired distance or formation configuration between the target and agent i. Furthermore, to deal with the uncertain dynamics and input constraints in many physical systems, the improved CSC algorithm is expected to be designed to meet the practical requirements. The following assumption about the graph between target and agents is given to guarantee the nonnegative of matrix H.

Assumption 2 Let $G_A = (V, \varepsilon, A)$ be the directed graph characterizing the interaction among the N agents with Laplacian matrix $L_A \in \mathbb{R}^{N\times N}$, $\bar{G} = (\bar{V}, \bar{\varepsilon}, \bar{A})$ be the directed graph characterizing the interaction between the target and the N agents, and $a_{i0} > 0$ if the agent i can obtain the position information of the target. We assume that the target has directed paths to all agents.

Lemma 1[4] If Assumption 2 holds true, the matrix $H = L_A + \mathrm{diag}(a_{10}, \ldots, a_{N0})$ has non-negative eigenvalues.

Remark 1 In practice, δ_{i0} can be reasonable, because the size, shape and volume of the target are usually known to a portion of agents by navigation or detection before they move together to surround the target, which plays an important role in realizing CSC and is the main difference from those in other references.

3. CSC algorithms design

In this section, two CSC algorithms are designed for agents to surround a static target. Firstly, we consider the EL systems in the presence of uncertain dynamics. Then, the constraints on control input and the absence of the relative velocity information are further considered.

3.1. Neural-network backstepping CSC for EL systems with uncertain dynamics

Construct the following auxiliary variable for the i-th agent

$$q_{ri} = -\beta \int_0^t \sum_{j=0}^{N} a_{ij}(q_i - q_j - \delta_{ij})\,\mathrm{d}\tau, \tag{2}$$

where δ_{ij} is the desired relative distance between agent i and j, and β is a positive constant. Then, we design the backstepping CSC based on NN. Backstepping-based method is an effective controller design tool for the nonlinear system.[36] Following the backstepping control design procedure, we define the error variables $Z_{1i}, Z_{2i} \in \mathrm{R}^p$ as

$$Z_{1i} = q_i - q_{ri} = q_i + \beta \int_0^t \sum_{j=0}^{N} a_{ij}(q_i - q_j - \delta_{ij})\,\mathrm{d}\tau, \tag{3}$$

$$Z_{2i} = \dot{q}_i - \alpha_{1i}, \tag{4}$$

where α_{1i} is a virtual variable which will be designed later.

Differentiating both sides of Eq. (3) yields

$$\dot{Z}_{1i} = Z_{2i} + \alpha_{1i} - \dot{q}_{ri}. \tag{5}$$

We choose the virtual control α_{1i} as

$$\alpha_{1i} = \dot{q}_{ri} - K_{1i}Z_{1i}, \tag{6}$$

where K_{1i} is a symmetric positive-definite matrix. Construct the first Lyapunov function V_{1i} as

$$V_{1i} = \frac{1}{2}Z_{1i}^{\mathrm{T}}Z_{1i}. \tag{7}$$

According to Eq. (6), we can obtain

$$\dot{V}_{1i} = -Z_{1i}^{\mathrm{T}}K_{1i}Z_{1i} + Z_{1i}^{\mathrm{T}}Z_{2i}. \tag{8}$$

Applying Eq. (4) to Eq. (1), we can obtain

$$M_i\dot{Z}_{2i} + C_iZ_{2i} = \tau_i + \omega_i - M_i\dot{\alpha}_{1i} - C_i\alpha_{1i} - g_i. \tag{9}$$

We construct the second Lyapunov function

$$V_{2i} = V_{1i} + \frac{1}{2}Z_{2i}^{\mathrm{T}}M_iZ_{2i}. \tag{10}$$

By using Property 1 and Eq. (9), we have

$$\begin{aligned}\dot{V}_{2i} &= -Z_{1i}^{\mathrm{T}}K_{1i}Z_{1i} + Z_{1i}^{\mathrm{T}}Z_{2i} + \frac{1}{2}Z_{2i}^{\mathrm{T}}\dot{M}_iZ_{2i} + Z_{2i}^{\mathrm{T}}M_i\dot{Z}_{2i}\\ &= -Z_{1i}^{\mathrm{T}}K_{1i}Z_{1i} + Z_{1i}^{\mathrm{T}}Z_{2i} + Z_{2i}^{\mathrm{T}}(\tau_i + \omega_i\\ &\quad - M_i\dot{\alpha}_{1i} - C_i\alpha_{1i} - g_i).\end{aligned} \tag{11}$$

We give the following control law for the i-th agent

$$\tau_i = M_i\dot{\alpha}_{1i} + C_i\alpha_{1i} + g_i - \omega_i - Z_{1i} - K_{2i}Z_{2i}, \tag{12}$$

where K_{2i} is a symmetric positive definite matrix. Then, substituting Eq. (12) into Eq. (11), we obtain

$$\dot{V}_{2i} = -Z_{1i}^{\mathrm{T}}K_{1i}Z_{1i} - Z_{2i}^{\mathrm{T}}K_{2i}Z_{2i}. \tag{13}$$

From Eq. (13), we can easily conclude that the system under control law (12) is asymptotically stable. However, the system parameters M_i, C_i, g_i, and disturbance ω_i are all used in control law (12), which are difficult to obtain in practice because of uncertain dynamics. To solve this problem, artificial neural network function approximation techniques, neural-networks (NN) are used to approximate the unknown nonlinear parametric uncertainties $f_i(q_i, \dot{q}_i, \dot{\alpha}_{1i}, \alpha_{1i}) = -M_i\dot{\alpha}_{1i} - C_i\alpha_{1i} - g_i$, which can be represented as

$$f_i(q_i, \dot{q}_i, \dot{\alpha}_{1i}, \alpha_{1i}) = W_i^{\mathrm{T}}\theta_i(q_i, \dot{q}_i, \dot{\alpha}_{1i}, \alpha_{1i}) + \varepsilon_i, \tag{14}$$

where W_i is the ideal constant approximation weight matrix, $\theta_i(\cdot)$ is the suitable basis set of functions, and ε_i is the approximation error for the i-th agent which is bounded by $\|\varepsilon_i\| \le \varepsilon_{Mi}$ where ε_{Mi} is a positive constant. In practice, the nonlinear function cannot be approximated exactly by NN. Thus, the estimate of $f_i(q_i, \dot{q}_i, \dot{\alpha}_{1i}, \alpha_{1i})$ can be expressed as

$$\hat{f}_i(q_i, \dot{q}_i, \dot{\alpha}_{1i}, \alpha_{1i}) = \hat{W}_i^{\mathrm{T}}\theta_i(q_i, \dot{q}_i, \dot{\alpha}_{1i}, \alpha_{1i}), \tag{15}$$

where $\hat{W}_i$ is the estimate of W_i.

Thus, to deal with the uncertain dynamics in the system, we propose the following CSC law:

$$\tau_i = -\hat{W}_i^{\mathrm{T}}\theta_i - Z_{1i} - K_{2i}Z_{2i} - k_1\mathrm{sgn}(Z_{2i}), \tag{16}$$

$$\dot{\hat{W}}_i = \gamma\theta_i Z_{2i}^{\mathrm{T}}, \tag{17}$$

where γ and k_1 are positive constants.

Theorem 1 Suppose that Assumptions 1 and 2 hold, considering an arbitrary agent in this system, say, i-th agent, in the presence of the uncertain dynamics, using Eq. (16) for τ_i in Eq. (1), we can conclude that the static target will be surrounded by all agents with the desired formation or relative distance δ_{i0}.

Proof Construct the third Lyapunov function as

$$V_{3i} = V_{2i} + \frac{1}{2\gamma}\mathrm{tr}(\tilde{W}_i^{\mathrm{T}}\tilde{W}_i), \tag{18}$$

where $\tilde{W}_i = W_i - \hat{W}_i$. Taking the derivative of V_{3i} using Eq. (11) gives

$$\begin{aligned}\dot{V}_{3i} \;=\; & -Z_{1i}^{\mathrm{T}}K_{1i}Z_{1i} + Z_{1i}^{\mathrm{T}}Z_{2i} + Z_{2i}^{\mathrm{T}}(\tau_i + \omega_i - M_i\dot{\alpha}_{1i} \\ & - C_i\alpha_{1i} - g_i) + \frac{1}{\gamma}\mathrm{tr}(\tilde{W}_i^{\mathrm{T}}\dot{\tilde{W}}_i).\end{aligned} \tag{19}$$

Substituting Eqs. (14), (16), and (17) into Eq. (19), we have

$$\begin{aligned}\dot{V}_{3i} \;=\; & -Z_{1i}^{\mathrm{T}}K_{1i}Z_{1i} + Z_{1i}^{\mathrm{T}}Z_{2i} + Z_{2i}^{\mathrm{T}}(-\hat{W}_i^{\mathrm{T}}\theta_i - Z_{1i} \\ & - K_{2i}Z_{2i} - k_1\mathrm{sgn}(Z_{2i}) + \omega_i \\ & + W_i^{\mathrm{T}}\theta_i + \varepsilon_i) + \frac{1}{\gamma}\mathrm{tr}(\tilde{W}_i^{\mathrm{T}}(-\gamma\theta_i Z_{2i}^{\mathrm{T}})) \\ =\; & -Z_{1i}^{\mathrm{T}}K_{1i}Z_{1i} - Z_{2i}^{\mathrm{T}}K_{2i}Z_{2i} + Z_{2i}^{\mathrm{T}}\tilde{W}_i^{\mathrm{T}}\theta_i - \mathrm{tr}(\tilde{W}_i^{\mathrm{T}}\theta_i Z_{2i}^{\mathrm{T}}) \\ & - k_1\|Z_{2i}\| + Z_{2i}^{\mathrm{T}}(\omega_i + \varepsilon_i).\end{aligned} \tag{20}$$

Because $Z_{2i}^{\mathrm{T}}\tilde{W}_i^{\mathrm{T}}\theta_i$ is a scalar, we can obtain $Z_{2i}^{\mathrm{T}}\tilde{W}_i^{\mathrm{T}}\theta_i = tr(Z_{2i}^{\mathrm{T}}\tilde{W}_i^{\mathrm{T}}\theta_i) = \mathrm{tr}(\tilde{W}_i^{\mathrm{T}}\theta_i Z_{2i}^{\mathrm{T}})$. Meanwhile,

$$Z_{2i}^{\mathrm{T}}(\omega_i + \varepsilon_i) \le \|Z_{2i}\|(\|\omega_i\| + \|\varepsilon_i\|) \le \|Z_{2i}\|(\|\omega_{Mi}\| + \|\varepsilon_{Mi}\|).$$

By choosing large enough k_1 such that $k_1 \ge \|\omega_{Mi}\| + \|\varepsilon_{Mi}\|$, we can obtain

$$\dot{V}_{3i} \le -Z_{1i}^{\mathrm{T}}K_{1i}Z_{1i} - Z_{2i}^{\mathrm{T}}K_{2i}Z_{2i}. \tag{21}$$

Because K_{1i} and K_{2i} are symmetrically positively definite, we can obtain that $\dot{V}_{3i} \le 0$ and $V_{3i}(t) \le V_{3i}(0)$, $\forall t \ge 0$. Therefore, $Z_{1i}(t)$, $Z_{2i}(t)$, and $\tilde{W}_i(t)$ are all bounded, which means that $Z_{1i}(t) \in \mathbb{L}_\infty$ and $Z_{2i}(t) \in \mathbb{L}_\infty$. From Eq. (4) and Property 2, we know that q_i, $\dot{q}_i$ and α_{1i}, $\dot{Z}_{1i}$, $\dot{Z}_{2i}$, and $\dot{\alpha}_{1i}$ are all bounded, which leads to $\dot{Z}_{1i} \in \mathbb{L}_\infty$ and $\dot{Z}_{2i} \in \mathbb{L}_\infty$. Integrating both sides of inequality (20), we have

$$\int_0^t (Z_{1i}^{\mathrm{T}}K_{1i}Z_{1i} + Z_{2i}^{\mathrm{T}}K_{2i}Z_{2i})\,\mathrm{d}\tau \le V_{3i}(0) - V_{3i}(t). \tag{22}$$

Thus, we can obtain $\dot{Z}_{1i} \in \mathbb{L}_2$ and $\dot{Z}_{2i} \in \mathbb{L}_2$. By using Barbalat's lemma, we have

$$\lim_{t\to\infty} Z_{1i}(t) = 0, \tag{23}$$

$$\lim_{t\to\infty} Z_{2i}(t) = 0. \tag{24}$$

Note that equations (3) and (4) can be written as

$$Z_{1i} = q_i - q_{ri} = q_i + \beta\int_0^t \sum_{j=0}^N a_{ij}(q_i - q_j - \delta_{ij})\,\mathrm{d}\tau \tag{25}$$

and

$$Z_{2i} = \dot{q}_i - \alpha_{1i} = \dot{q}_i - \dot{q}_{ri} + K_{1i}Z_{1i} = \dot{Z}_{1i} + K_{1i}Z_{1i}. \tag{26}$$

Sustituting Eqs. (25) and (26) into Eqs. (23) and (24), we can obtain

$$\lim_{t\to\infty}\dot{Z}_{1i} = \lim_{t\to\infty}[\dot{q}_i + \beta\sum_{j=0}^N a_{ij}(q_i - q_j - \delta_{ij})] = 0. \tag{27}$$

According to the results in Ref. [37], we conclude that if the directed graph contains a spanning tree and the desired distance δ_{ij} is feasible, there is constant vector $\delta_{i0}, i = 1,\ldots,N$ such that $\delta_{ij} = \delta_{i0} - \delta_{j0}$. Define vector $\dot{Z}_1 = [\dot{Z}_{11}^{\mathrm{T}},\ldots,\dot{Z}_N^{\mathrm{T}}]^{\mathrm{T}}$, $q = [q_1^{\mathrm{T}},\ldots,q_N^{\mathrm{T}}]^{\mathrm{T}}$, and $\delta_0 = [\delta_{10}^{\mathrm{T}},\ldots,\delta_{N0}^{\mathrm{T}}]^{\mathrm{T}}$. For $\forall i \in M$, equation (27) holds true. Thus, equation (27) can be written as

$$\dot{Z}_1 = \dot{q} + \beta[H \otimes I_p](q - 1_N \otimes q_0 - 1_N \otimes \delta_0). \tag{28}$$

By Lemma 1, we can obtain the following conclusion:

$$\lim_{t\to\infty} q - 1_N \otimes q_0 - 1_N \otimes \delta_0 = 0, \tag{29}$$

which leads to

$$\lim_{t\to\infty}(q_i - q_0 - \delta_{i0}) = 0. \tag{30}$$

This completes the proof of Theorem 1.

3.2. Command-filtered backstepping CSC for EL systems with input constraints

In Subsection 3.1, we design a CSC algorithm for a multiple EL system with uncertain dynamics. However, the input constraints in the system are not considered, which cannot be ignored in the presence of limitation of actuator in practice. Inspired by Refs. [32] and [38], the command filter (CF) can be used to solve the problem of input constraints in the system. As a byproduct in this study, the absence of relative velocity information in directed graph is also handled by the differential output of CF.

The structure of CF is shown in Fig. 1. When input signal is x_{c}^0, CF can filter the input signal x_{c}^0 to produce a magnitude, rate and bandwidth-limited signal x_{c} and its derivation $\dot{x}_{\mathrm{c}}$, which means that the derivative $\dot{x}_{\mathrm{c}}$ is computed without any differentiation but with integration.

The transfer function from the variable x_{c}^0 to the output x_{c} can be derived as

$$\frac{X_{\mathrm{c}}(s)}{X_{\mathrm{c}}^0(s)} = \frac{\omega_n^2}{s + 2\varsigma\omega_n s + \omega_n^2}. \tag{31}$$

From Ref. [32], we have the lemma about the CF as follows.

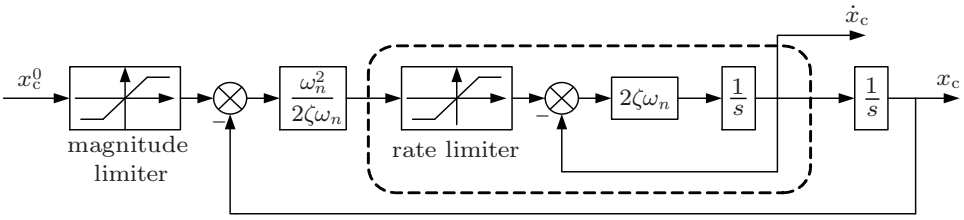


Fig. 1. Structure of a command filter.

Lemma 2[32] The CF can filter the input signal x_c^0 to produce a magnitude, rate and bandwidth-limited signal x_c and its derivative $\dot{x}_c$, which means

$$x_c(t,\varepsilon) - x_c^0 = O(\varepsilon), \tag{32}$$
$$\dot{x}_c(t,\varepsilon) - x_c^0 = O(\varepsilon), \tag{33}$$

where $\varepsilon = 1/\omega_n$ and $O(\varepsilon)$ denotes the infinitesimal of higher order about ε. Inspired by the above two advantages of CF, we will design a CSC algorithm by using two command filters to cope with the constraints on control input and the absence of the relative velocity information in directed graph.

Firstly, define the following compensated error vector:

$$\tilde{Z}_{1i} = Z_{1i} - \psi_{1i}, \tag{34}$$
$$\tilde{Z}_{2i} = Z_{2i} - \psi_{2i} = \dot{q}_i - \alpha_{1i} - \psi_{2i}, \tag{35}$$

where ψ_{1i} and ψ_{2i} are auxiliary variables, which will be designed later. Constructing the Lyapunov function as

$$V_{4i} = \frac{1}{2}\tilde{Z}_{1i}^{\mathrm{T}}\tilde{Z}_{1i} + \frac{1}{2}\tilde{Z}_{2i}^{\mathrm{T}}M_i(q_i)\tilde{Z}_{2i} + \frac{1}{2\gamma}\mathrm{tr}(\tilde{W}_i^{\mathrm{T}}\tilde{W}_i). \tag{36}$$

The derivative of Eq. (36) follows

$$\begin{aligned}\dot{V}_{4i} \;=\; & \tilde{Z}_{1i}^{\mathrm{T}}\dot{\tilde{Z}}_{1i} + \tilde{Z}_{2i}^{\mathrm{T}}M_i(q_i)\dot{\tilde{Z}}_{2i} \\ & + \frac{1}{2}\tilde{Z}_{2i}^{\mathrm{T}}\dot{M}_i(q_i)\tilde{Z}_{2i} + \frac{1}{\gamma}\mathrm{tr}(\tilde{W}_i^{\mathrm{T}}\dot{\tilde{W}}_i).\end{aligned} \tag{37}$$

Because

$$\dot{\tilde{Z}}_{1i} = \dot{q}_i - \dot{q}_{ri} - \dot{\psi}_{1i} = Z_{2i} + \alpha_{1i} - \dot{q}_{ri} - \dot{\psi}_{1i}, \tag{38}$$
$$\begin{aligned}M_i(q_i)\dot{\tilde{Z}}_{2i} &= M_i(q_i)(\dot{Z}_{2i} - \dot{\psi}_{2i}) \\ &= \tau_i + \omega_i - M_i\dot{\alpha}_{1i} - C_i\alpha_{1i} - C_iZ_{2i} - g_i + M_i\psi_{2i}.\end{aligned} \tag{39}$$

Design the adaptive law as

$$\dot{\psi}_{1i} = \alpha_{1i} - \dot{q}_{ri} + K_{3i}\tilde{Z}_{1i} + \psi_{2i}, \tag{40}$$
$$\dot{\psi}_{2i} = M_i^{-1}(\tau_{\mathrm{o}i} - \tau_i), \tag{41}$$

where $\tau_{\mathrm{o}i}$ is the input of the first CF which will be designed later, τ_i is the output of the first CF which is magnitude, rate and bandwidth-limited and will be applied to the actual system.

Applying Eqs. (38)–(41) to Eq. (30), we can obtain

$$\begin{aligned}\dot{V}_{4i} = & -\tilde{Z}_{1i}^{\mathrm{T}}K_{3i}\tilde{Z}_{1i} + \tilde{Z}_{1i}^{\mathrm{T}}\tilde{Z}_{2i} + \tilde{Z}_{2i}^{\mathrm{T}}(\tau_i - \tau_i + \tau_{\mathrm{o}i} - f_i + \omega_i) \\ & + \frac{1}{\gamma}\mathrm{tr}(\tilde{W}_i^{\mathrm{T}}\dot{\tilde{W}}_i).\end{aligned} \tag{42}$$

Then, we design the following CSC algorithm:

$$\tau_{\mathrm{o}i} = -\tilde{Z}_{1i} - K_{4i}\tilde{Z}_{2i} - \hat{W}_i^{\mathrm{T}}\theta_i - k_1\mathrm{sgn}(\tilde{Z}_{2i}), \tag{43}$$
$$\dot{\hat{W}}_i = \gamma\theta_i\tilde{Z}_{2i}^{\mathrm{T}}. \tag{44}$$

Substituting Eq. (43) into Eq. (42), we can obtain

$$\begin{aligned}\dot{V}_{4i} &= -\tilde{Z}_{1i}^{\mathrm{T}}K_{3i}\tilde{Z}_{1i} - \tilde{Z}_{2i}^{\mathrm{T}}K_{4i}\tilde{Z}_{2i} + \tilde{Z}_{2i}^{\mathrm{T}}(\omega_i + \varepsilon_i) - k_1\left\|\tilde{Z}_{2i}\right\| \\ &\le -\tilde{Z}_{1i}^{\mathrm{T}}K_{3i}\tilde{Z}_{1i} - \tilde{Z}_{2i}^{\mathrm{T}}K_{4i}\tilde{Z}_{2i} \\ &\quad + \left\|\tilde{Z}_{2i}\right\|(\|\omega_i\| + \|\varepsilon_i\|) - k_1\left\|\tilde{Z}_{2i}\right\|.\end{aligned} \tag{45}$$

By using $k_1 \ge \|\omega_{Mi}\| + \|\varepsilon_{Mi}\| \ge \|\omega_i\| + \|\varepsilon_i\|$, we can conclude

$$\dot{V}_{4i} \le -\tilde{Z}_{1i}^{\mathrm{T}}K_{3i}\tilde{Z}_{1i} - \tilde{Z}_{2i}^{\mathrm{T}}K_{4i}\tilde{Z}_{2i} \le 0. \tag{46}$$

Like the statements in Subsection 3.1, we can obtain

$$\lim_{t\to\infty}\tilde{Z}_{1i}(t) = 0, \tag{47}$$
$$\lim_{t\to\infty}\tilde{Z}_{2i}(t) = 0. \tag{48}$$

From Eqs. (47) and (48), we can easily obtain the conclusion of asymptotical stability of the system with input constraints. However, the adaptive law (41) uses the system inertia matrix M_i, which is difficult to accurately obtain because of uncertain dynamics. At the same time, the relative velocity information is also used in $\dot{\alpha}_{1i}$ in Eq. (15), which requires the system to be equipped with a velocity sensor. To tackle the first problem, we assume that $M_i = M_{\mathrm{o}i} + \Delta M_i$ where $M_{\mathrm{o}i}$ is the nominal value and ΔM_i is the bounded uncertain part. To solve the second problem, we fully use the differential output of the CF. Thus, we propose the adjusted CSC algorithm

$$\dot{\psi}_{2i} = \dot{\Omega}_i + M_{\mathrm{o}i}^{-1}(\tau_{\mathrm{o}i} - \tau_i), \tag{49}$$
$$\tau_{\mathrm{o}i} = -\tilde{Z}_{1i} - K_{4i}\tilde{Z}_{2i} + \hat{W}_{\mathrm{o}i}^{\mathrm{T}}\theta_{\mathrm{o}i} - k_2\mathrm{sgn}(\tilde{Z}_{2i}), \tag{50}$$
$$\dot{\hat{W}}_{\mathrm{o}i} = \gamma\theta_{\mathrm{o}i}\tilde{Z}_{2i}^{\mathrm{T}}, \tag{51}$$

where α_{1i} is the input of the second CF, $\dot{\Omega}_i$ is the output of the second CF which converges to $\dot{\alpha}_{1i}$, and $f_{\mathrm{o}i}(q_i,\dot{q}_i,\alpha_{1i},\dot{\Omega}_i) = M_i\dot{\Omega}_i + C_i\alpha_{1i} + g_i$ is approximated by NN which can be represented as

$$f_{\mathrm{o}i}(q_i,\dot{q}_i,\alpha_{1i},\dot{\Omega}_i) = W_{\mathrm{o}i}^{\mathrm{T}}\theta_{\mathrm{o}i}(q_i,\dot{q}_i,\alpha_{1i},\dot{\Omega}_i) + \varepsilon_{\mathrm{o}i}. \tag{52}$$

Like that in Subsection 3.1, ε_{oi} is bounded and the estimate of $f_{oi}(q_i,\dot{q}_i,\alpha_{1i},\dot{\Omega}_i)$ can be written as $\hat{f}_{oi}(q_i,\dot{q}_i,\alpha_{1i},\dot{\Omega}_i)=\hat{W}_{oi}^{\mathrm{T}}\theta_{oi}(q_i,\dot{q}_i,\alpha_{1i},\dot{\Omega}_i)$.

Theorem 2 Suppose that Assumptions 1 and 2 hold, considering an arbitrary agent in the system, say, the i-th agent, in the presence of the uncertain dynamics and input constraints, using Eq. (50) for Eq. (1), we can obtain that the static target will be surrounded by all agents with the desired formation or relative distance δ_{i0}.

Proof Construct the Lyapunov function as

$$V_{5i}=\frac{1}{2}\tilde{Z}_{1i}^{\mathrm{T}}\tilde{Z}_{1i}+\frac{1}{2}\tilde{Z}_{2i}^{\mathrm{T}}M_i(q_i)\tilde{Z}_{2i}+\frac{1}{2\gamma}\mathrm{tr}(\tilde{W}_i^{\mathrm{T}}\tilde{W}_i). \tag{53}$$

Applying Eq. (50) to Eq. (39), we can obtain

$$\begin{aligned}M_i\dot{\tilde{Z}}_{2i}=M_i(\dot{Z}_{2i}-\dot{\psi}_{2i})=\tau_i+\omega_i-M_i(q_i)\dot{\alpha}_{1i}-C_i(q_i,\dot{q}_i)\alpha_{1i}\\-C_i(q_i,\dot{q}_i)Z_{2i}-g_i+(M_{oi}+\Delta M_i)\dot{\psi}_{2i}.\end{aligned} \tag{54}$$

By similar statements, we have

$$\begin{aligned}\dot{V}_{5i}=-\tilde{Z}_{1i}^{\mathrm{T}}K_{3i}\tilde{Z}_{1i}-\tilde{Z}_{2i}^{\mathrm{T}}K_{4i}\tilde{Z}_{2i}+\tilde{Z}_{2i}^{\mathrm{T}}(\Delta M_i\dot{\psi}_{2i}+\omega_i+\varepsilon_i)\\-k_2\left\|\tilde{Z}_{2i}\right\|+\tilde{Z}_{2i}^{\mathrm{T}}(M_i\dot{\alpha}_{1i}-M_i\dot{\Omega}_i).\end{aligned} \tag{55}$$

By using Property 2, we can obtain

$$\begin{aligned}\dot{V}_{5i}\le&-\tilde{Z}_{1i}^{\mathrm{T}}K_{3i}\tilde{Z}_{1i}-\tilde{Z}_{2i}^{\mathrm{T}}K_{4i}\tilde{Z}_{2i}\\&-(k_2-\|\Delta M_i\dot{\psi}_{2i}\|-\|\omega_i\|\\&-\|\varepsilon_i\|-k_{\bar{m}}O(\varepsilon))\left\|\tilde{Z}_{2i}\right\|,\end{aligned} \tag{56}$$

where $\dot{\psi}_{2i}$ is bounded as it is related to CFs. Let $k_2\ge\|\Delta M_i\dot{\psi}_{2i}\|+\|\omega_{Mi}\|+\|\varepsilon_{Mi}\|+k_{\bar{m}}O(\varepsilon)$, we can obtain that

$$\dot{V}_{5i}\le-\tilde{Z}_{1i}^{\mathrm{T}}K_{3i}\tilde{Z}_{1i}-\tilde{Z}_{2i}^{\mathrm{T}}K_{4i}\tilde{Z}_{2i}\le 0. \tag{57}$$

Like the statements in Subsection 3.1, we can conclude

$$\lim_{t\to\infty}\tilde{Z}_{1i}(t)=0, \tag{58}$$

$$\lim_{t\to\infty}\tilde{Z}_{2i}(t)=0. \tag{59}$$

Finally, it comes to the conclusion of asymptotical stability of the system, which completes the proof of Theorem 2.

Remark 2 From the proof of Theorem 2, we can obtain $\lim_{t\to\infty}\tilde{Z}_{1i}(t)=0$ and $\lim_{t\to\infty}\tilde{Z}_{2i}(t)=0$ for the system with uncertain dynamics and input constraints. However, we cannot directly obtain $\lim_{t\to\infty}Z_{1i}(t)=0$ and $\lim_{t\to\infty}Z_{2i}(t)=0$ because ψ_{1i} and ψ_{2i} are not zero. According to Ref. [32], the control inputs are usually so aggressive during the initial stage that the magnitude, rate, or bandwidth limits will come into effect. As a result, the CF cannot completely track the inputs. With the ψ_{1i} and ψ_{2i} compensating for the tracking errors of the CF input and output, the limits will eventually be ineffective. Finally, the ψ_{1i} and ψ_{2i} variables converge to zero, and Z_{1i} and Z_{2i} converges to $\tilde{Z}_{1i}$ and $\tilde{Z}_{2i}$, respectively.

Remark 3 The above designed CSC algorithms are mainly used to surround the single target. However, it is easy to extend these two CSC algorithms to surround multiple targets, which depends on the planning of the desired formation configuration δ_{i0}. In other words, as long as the desired relative distance δ_{i0} between the agent i and the average position of all targets is longer than the convex hull spanned by all targets, the designed two CSC algorithms will still be effective.

4. Simulation examples

In this section, we present a numerical simulation to verify the effectiveness of the proposed CSC algorithms in this study. With the consideration of a group of eight satellites (numbered as 1 to 8) surrounding a stationary target (numbered as 0), the equations of relative orbit motion in the local-vertical, local-horizontal (LVLH) rotating frame with a chief satellite can be described as[39]

$$\begin{aligned}&\ddot{x}_i-2\omega_0\dot{y}_i-\omega_0^2x_i-\dot{\omega}_0y_i+\frac{\mu_{\mathrm{e}}(R_0+x_i)}{R_i^3}-\frac{\mu_{\mathrm{e}}}{R_0^2}\\&=\frac{\tau_{oix}+\tau_{\mathrm{do}ix}}{m_i},\end{aligned} \tag{60}$$

$$\begin{aligned}&\ddot{y}_i^2+2\omega_0\dot{x}_i-\omega_0^2y_i+\dot{\omega}_0x_i+\frac{\mu_{\mathrm{e}}y_i}{R_i^3}\\&=\frac{\tau_{oiy}+\tau_{\mathrm{do}iy}}{m_i},\end{aligned} \tag{61}$$

$$\ddot{z}_i+\frac{\mu_{\mathrm{e}}z_i}{R_i^3}=\frac{\tau_{oiz}+\tau_{\mathrm{do}iz}}{m_i}, \tag{62}$$

where $[x_i,y_i,z_i]$ are the relative coordinates of the i-th satellite in the LVLH frame, R_0 is the orbit radius, m_i is the mass of the i-th satellite, μ_{e} is the gravitation constant, $\omega_0=\sqrt{\mu_{\mathrm{e}}/R_0^3}$ is the orbit angular velocity, R_i is the distance between the satellite and the geocenter, $[\tau_{oix},\tau_{oiy},\tau_{oiz}]$ are the control forces, and $[\tau_{\mathrm{do}ix},\tau_{\mathrm{do}iy},\tau_{\mathrm{do}iz}]$ are the uncertain dynamics and disturbance perturbations. Noting that the above relative orbit motion equations can be transformed into Euler–Lagrange system

$$m_i\ddot{q}_i+C_i\dot{q}_i+g_i=\tau_{oi}+\tau_{\mathrm{do}i}, \tag{63}$$

in which, $q_i=[x_i,\ y_i,\ z_i]^{\mathrm{T}}$, $\tau_{oi}=[\tau_{oix},\ \tau_{oiy},\ \tau_{oiz}]^{\mathrm{T}}$, $\tau_{\mathrm{do}i}=[\tau_{\mathrm{do}ix},\ \tau_{\mathrm{do}iy},\ \tau_{\mathrm{do}iz}]^{\mathrm{T}}$, $C_i=2m_i\begin{bmatrix}0&-\omega_0&0\\\omega_0&0&0\\0&0&0\end{bmatrix}$, and

$$g_i=m_i\begin{bmatrix}-\omega_0x_i-\dot{\omega}_0y_i+\mu_{\mathrm{e}}(R_0+x_i)/R_i^3-\mu_{\mathrm{e}}/R_0^2\\-\omega_0y_i+\mu_{\mathrm{e}}y_i/R_i^3+\dot{\omega}_0x_i\\\mu_{\mathrm{e}}z_i/R_i^3\end{bmatrix}.$$

We assume that the relative orbit reference of the CSC system follows a near-circular orbit with the initial orbit elements $[ae\ i\ \Delta\ \omega\ f]=[7136.0\ 0.00160^\circ\ 10^\circ\ 30^\circ\ 0^\circ]$ where

a is the semi-major axis(km) of the reference orbit, e is the eccentricity, i is the inclination, Δ is the longitude of the ascending node, ω is the argument of periapsis, and f is the true anomaly. For each satellite i ($\forall i \in \{1,\ldots,8\}$), $m_i = 35$ kg and $\tau_{\mathrm{do}i} = [-1.025\sin(t), 6.248\cos(t), 1]^{\mathrm{T}} \times 10^{-4}$ N. The directed communication graph among eight satellites and the static target is shown in Fig. 2.

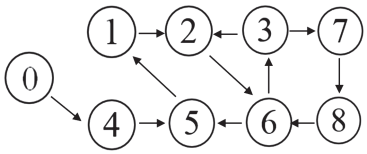


Fig. 2. The communication topology among the satellites and the target.

For each satellite ($\forall i = 1,\ldots,8$), the target ($i = 0$) has at least one directed path to each satellite (for example, to agent 6, there is a directed path: $0 \to 4 \to 5 \to 1 \to 2 \to 6$). Therefore, this communication topology satisfies Assumption 2. The Laplacian matrix of the agents is composed of

$$L_A = \begin{bmatrix} 1 & 0 & 0 & 0 & -1 & 0 & 0 & 0 \\ -1 & 2 & -1 & 0 & 0 & 0 & 0 & 0 \\ 0 & 0 & 1 & 0 & 0 & -1 & 0 & 0 \\ 0 & 0 & 0 & 0 & 0 & 0 & 0 & 0 \\ 0 & 0 & 0 & -1 & 2 & 1 & 0 & 0 \\ 0 & -1 & 0 & 0 & 0 & 2 & 0 & -1 \\ 0 & 0 & -1 & 0 & 0 & 0 & 1 & 0 \\ 0 & 0 & 0 & 0 & 0 & 0 & -1 & 1 \end{bmatrix}.$$

We define $a_{40} = 1$ and $a_{k0} = 0$ ($k = 1,2,3,5,\ldots,8$). The desired relative distances are $\delta_{40} = [-50,-50,50]^{\mathrm{T}}$ m, $\delta_{15} = [0,0,100]^{\mathrm{T}}$ m, $\delta_{21} = [0,100,0]^{\mathrm{T}}$ m, $\delta_{23} = [100,0,0]^{\mathrm{T}}$ m, $\delta_{36} = [-100,0,100]^{\mathrm{T}}$ m, c, $\delta_{56} = [0,-100,0]^{\mathrm{T}}$ m, $\delta_{62} = [0,0,-100]^{\mathrm{T}}$ m, $\delta_{73} = [0,0,-100]^{\mathrm{T}}$ m, $\delta_{87} = [0,-100,0]^{\mathrm{T}}$ m, and $\delta_{68} = [100,100,0]^{\mathrm{T}}$ m, respectively. The initial states of satellites and target are $q_i(0) = [0,0,0]^{\mathrm{T}}$ m, $\dot{q}_i(0) = [0,0,0]^{\mathrm{T}}$ m/s, $q_0 = [200,200,200]^{\mathrm{T}}$ m, respectively.

The activation function of NN for the i-th satellite used in this simulation can be denoted as follows:

$$\varphi_i(z) = [\varphi_{i1}(z),\ldots,\varphi_{i6}(z)]^{\mathrm{T}}, \tag{64}$$

where $\varphi_{ij}(z)$ is a Gaussian function

$$\varphi_{ij}(z) = \exp\left(-\frac{\|z - c_{ij}\|^2}{\sigma_{ij}^2}\right), \quad j = 1,\ldots,6, \tag{65}$$

where $z = [q_i, \dot{q}_i, \alpha_{1i}, \dot{\alpha}_{1i}]^{\mathrm{T}} \in \mathbb{R}^{12}$. It is assumed that all the activation function of NN in the simulation is the same, c_{ij} represents the center of the receptive field which is evenly distributed in $[-5,5]^6 \times [-0.5,0.5]^6$, $\sigma_{ij} = 2$ is the width of Gaussian function, the initial NN weight matrix elements are all zeros which are denoted as $\hat{W}_i(0) = 0_{6\times 3}$.

To compare and illustrate the effectiveness and the advantages of the proposed CSC algorithms, we simulate the following three CSC algorithms: nominal CSC (NCSC) law (12), neural-networks CSC (NNCSC) law (16), and command filtered CSC (CFCSC) law (50) with four examples and the results are given below.

Example 1 NCSC for system with uncertain dynamics

The NCSC law can be described as

$$\tau_{\mathrm{o}i} = m_i\dot{\alpha}_{1i} + C_i\alpha_{1i} + g_i - Z_{1i} - K_{2i}Z_{2i}.$$

Uncertain dynamics: $\Delta_i = 0.05 \times (m_i\dot{\alpha}_{1i} + C_i\alpha_{1i} + g_i) - \tau_{\mathrm{do}i}$.

Controller parameters: $K_{1i} = 4I_3$, $K_{2i} = 4I_3$, $\beta = 0.01$.

Simulation results are shown in Fig. 3 and 4.

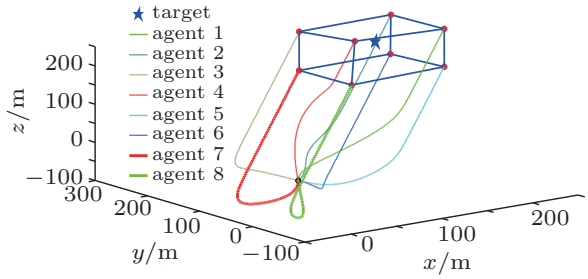


Fig. 3. (color online) Trajectories of agents using NCSC.

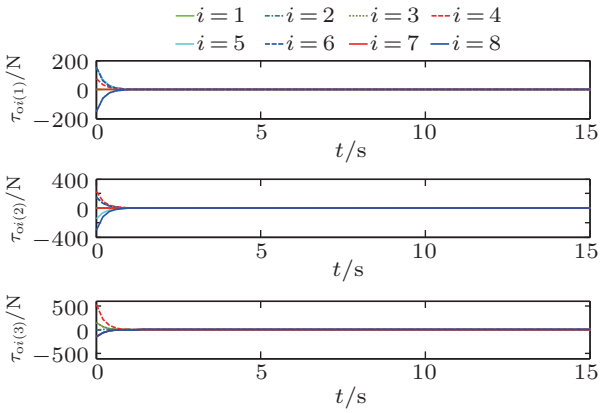


Fig. 4. (color online) Control forces of agents using NCSC.

Example 2 NNCSC for system with uncertain dynamics

Uncertain dynamics: m_i, C_i, g_i, and $\tau_{\mathrm{do}i}$ are all unknown. Controller parameters are taken as follows: $K_{1i} = 4I_3$, $K_{2i} = 4I_3$, $\beta = 0.01$, $\gamma = 1$, and $k = 0.1$.

Simulation results can be found in Fig. 5 and 6.

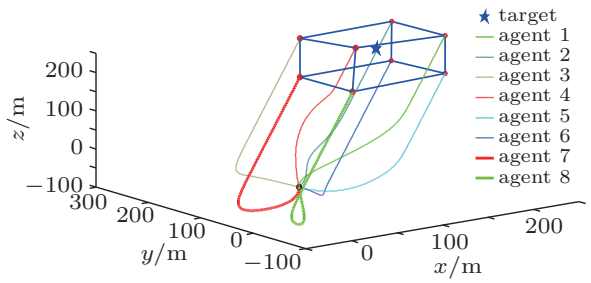


Fig. 5. (color online) Trajectories of agents using NNCSC.

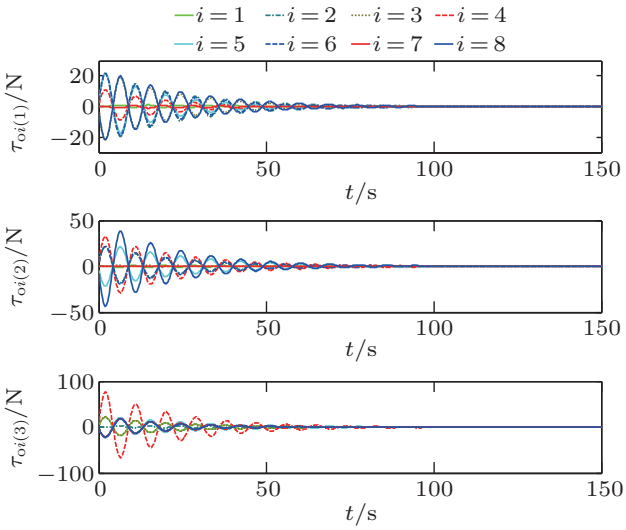


Fig. 6. (color online) Control forces of agents using NNCSC.

Example 3 NNCSC for system with uncertain dynamics and input constraints

Uncertain dynamics: m_i, C_i, g_i, and τ_{doi} are all unknown.

Input constraints: control saturation with upper limitation of 30 N.

Controller parameters: $K_{1i} = 4I_3$, $K_{2i} = 4I_3$, $\beta = 0.01$, $\gamma = 1$, and $k = 0.1$.

Simulation results are presented in Fig. 7 and 8.

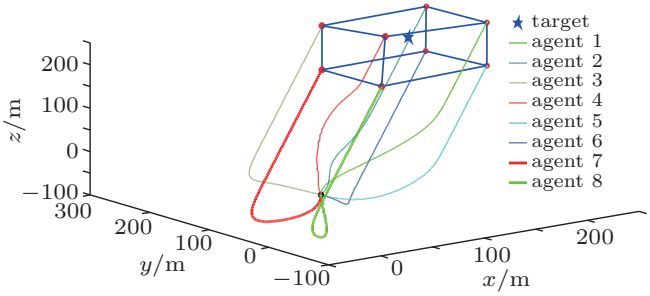


Fig. 7. (color online) Trajectories of agents using NNCSC.

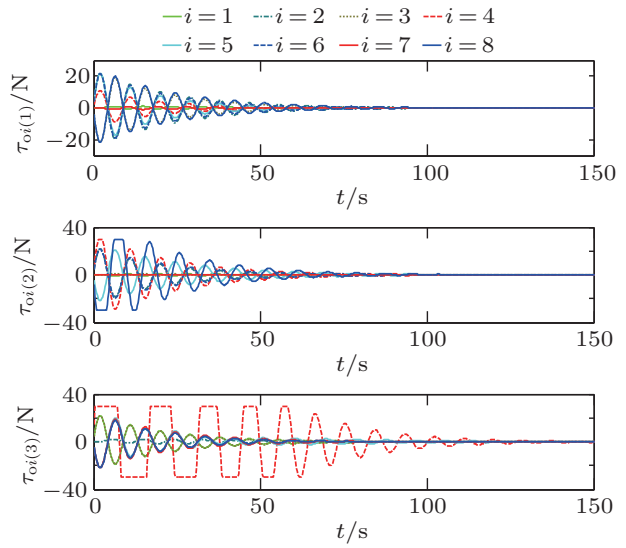


Fig. 8. (color online) Control forces of agents using NNCSC.

Example 4 CFCSC for system with uncertain dynamics and input constraints

Uncertain dynamics: m_i, C_i, g_i, and τ_{doi} are all unknown.

Input constraints: control saturation with upper limitation of 10 N.

Controller parameters: $K_{1i} = 0.002I_3$, c, $K_{4i} = 0.002I_3$, $\beta = 0.01$, $\gamma = 1$, $k = 50$, $\omega_n = 5\sqrt{6}$, and $\varepsilon = \sqrt{6}/6$.

Simulation results are displayed in Fig. 9, 10, and 11.

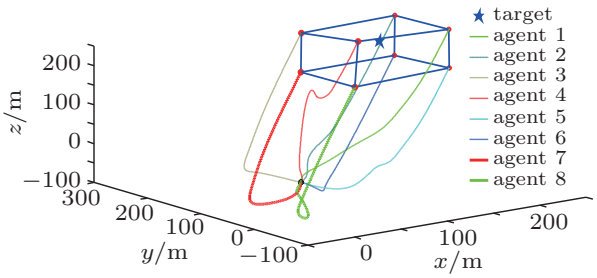


Fig. 9. (color online) Trajectories of agents using CFCSC.

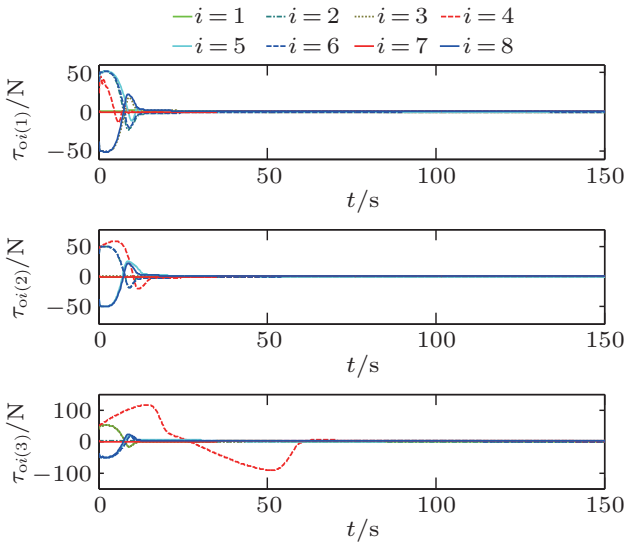


Fig. 10. (color online) Control inputs of CF of agents using CFCSC.

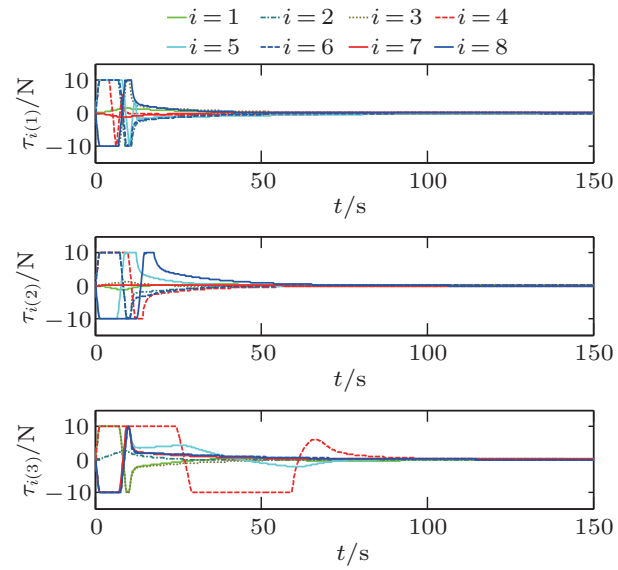


Fig. 11. (color online) Control outputs of CF of agents using CFCSC.

We can see that the eight satellites can surround the stationary target in the above four simulation examples. The comparisons of performances among these four CSC algorithms are given below.

Comparing Example 1 with Example 2, we can obtain that the convergence time of NCSC is ten times shorter than that of NNCSC, however, the control force amplitude of the NCSC is four times larger than that of NNCSC which is difficult to realize for the limitation to actuators. This demonstrates the effectiveness of NN in solving the system uncertain dynamics.

From the comparison between Example 2 and Example 3, we conclude that the input constraints will extend the convergence time of the system. From Example 3 of the simulation, we find that the saturation upper limitation of 30 N is nearly the maximum tolerance of the stability in system, however, this upper limitation may still be larger than the actual system output. This comparison shows the influences of the input constraints on the system stability and convergence time.

From Examples 3 and 4, we can obtain that with the absence of relative velocity information in directed graph and the constant gain k_2 larger than k_1, the amplitude of CFCSC is twice as large as that of NNCSC, however, by using command filter with a saturation upper limitation of 10 N, the stability of CSC system can still be guaranteed. This comparison demonstrates the utility of solving input constraints by command filter.

All of the above simulation analyses illustrate the effectiveness of the proposed two CSC algorithms and show the respective advantages of these four CSC laws.

5. Conclusions

Cooperatively surrounding controls for multiple nonlinear Euler–Lagrange systems with uncertain dynamics and input constraints are studied. By fully using the relative formation distance between agents, the cooperatively surrounding control problem is solved in a different and improved way. By incorporating neural-networks into backstepping control design framework, the uncertain dynamics in the system is handled. Then, a cooperatively surrounding control algorithm is designed for the agents such that all agents can move collectively to surround the stationary target. With the consideration of the limited control force output and the difficulty in measuring relative velocity, a command filtered backstepping cooperatively surrounding control algorithm is further developed. Future work will focus on the dynamic target and the collision avoidance.

References

[1] Mishne D 2004 *Journal of Guidance Control & Dynamics* **27** 685
[2] Yu W, Chen G, Wang Z and Yang W 2009 *IEEE Transactions on Systems Man & Cybernetics Part B Cybernetics* **39** 1568
[3] Peng Z, Wen G, Rahmani A and Yu Y 2013 *Robotics & Autonomous Systems* **61** 988
[4] Li Y M and Guan X P 2009 *Chin. Phys. B* **18** 3355
[5] Olfati-Saber R and Murray R M 2004 *IEEE Trans. Autom. Control* **49** 1520
[6] Ren W and Beard R W 2008 *Distributed Consensus in Multi-vehicle Cooperative Control*, Vol. 1 (New-York: Springer-Verlag) p. 25
[7] Zhang H G, Feng T, Yang G H and Liang H J 2015 *IEEE Trans. Cybern.* **45** 1315
[8] Mei J, Ren W and Ma G 2011 *IEEE Trans. Autom. Control* **56** 1415
[9] Zhang H G, Zhang J L, Yang G H and Luo Y H 2015 *IEEE Trans. Fuzzy Sys.* **23** 152
[10] Cao Y and Ren W 2012 *IEEE Trans. Autom. Control* **57** 33
[11] Zhang H G, Liang H J, Wang Z S and Feng T 2015 *IEEE Trans. Networks Learn. Sys.* Vol. pp, issue 99
[12] Zhao Y, Duan Z, Wen G and Chen G 2016 *Automatica* **64** 86
[13] Mei J, Ren W and Ma G 2012 *Automatica* **48** 653
[14] Ji M, Ferrari-Trecate G, Egerstedt M and Buffa A 2008 *IEEE Trans. Autom. Control* **53** 1972
[15] Notarstefano G, Egerstedt M and Haque M 2011 *Automatica* **47** 1035
[16] Lan Y, Yan G and Lin Z 2010 *Systems & Control Lett.* **59** 381
[17] Shames I, Dasgupta S, Fidan B and Anderson BDO 2012 *IEEE Trans. Autom. Control* **57** 889
[18] Tewari A 2013 *Journal of Spacecraft & Rockets* **50** 394
[19] Kim T H and Sugie T 2007 *Automatica* **43** 1426
[20] Chen F, Ren W and Cao Y 2010 *Systems & Control Lett.* **59** 704
[21] Wei T T and Chen X P 2014 *Chin. Phys. B* **23** 050201
[22] Shi Y J, Li R and Wei T T 2013 *Int. J. Sys. Sci.* **46** 1
[23] Kim T, Hara S and Hori Y 2010 *Int. J. Control* **83** 2040
[24] Kim T H and Sugie T 2007 *Automatica* **43** 1426
[25] Wang J R, Wang J P, He Z and Xu H T 2015 *Chin. Phys. B* **24** 060101
[26] Guan J B 2010 *Chin. Phys. Lett.* **27** 020502
[27] Li W and Zhang J F 2014 *Automatica* **50** 3231
[28] Shen Q and Shi P 2015 *Automatica* **53** 1204
[29] Gao S G, Dong H R, Ning B, Roberts C, Chen L and Sun X B 2015 *Chin. Phys. B* **24** 090506
[30] Hou J, Yan G F and Fan Z 2011 *Chin. Phys. B* **20** 048103
[31] Fu Z M, Liu L P and Song X N 2012 *Chin. Phys. B* **21** 118701
[32] Farrell J, Sharma M and Polycarpou M 2005 *Journal of Guidance Control & Dynamics* **28** 1089
[33] Hu Z, Ma C, Zhang L, Halme A and Hayat T 2015 *Neurocomputing* **147** 291
[34] Li Z, Ge S S, Adams M and Wijesoma W S 2008 *Automatica* **44** 776
[35] Du H, Li S and Qian C 2011 *IEEE Trans. Autom. Control* **56** 2711
[36] Wang X Y and Zhang H 2013 *Chin. Phys. B* **22** 048902
[37] Dimarogonas D V and Kyriakopoulos K J 2008 *Automatica* **44** 2648
[38] Lv Y Y, Hu Q L and Ma G F 2011 *Isa Trans.* **50** 573
[39] Alfriend K T, Vadali S R, Gurfil P, How J and Breger L S 2009 *Dynamics, Control and Navigation* **23** 385